Escuela de Caminos
Escuela Técnica Superior de Ingenieros de Caminos, Canales y Puertos
UPC BARCELONATECH

TRABAJO FINAL DE MASTER

THE DEVELOPMENT OF A REMOTE SENSING ALGORITHM FOR DIMETHYLSULPHIDE (DMS) IN THE SURFACE OF THE SOUTHERN OCEAN

Trabajo realizado por:
Nadia Milders

Dirigido por:
Manuel Espino, Martí Galí, Rafel Simó

Máster en:
Ingeniería Ambiental

Barcelona, 15 de Septiembre, 2021

Departamento de Ingeniería Civil y Ambiental

Abstract

Dimethylsulphide (DMS) is a marine biogenic gas which can modulate climate through increasing aerosol light scattering in the atmosphere and seeding cloud formation. In the Southern Ocean the climate is particularly sensitive to DMS, however these effects cannot be adequately quantified due to lack of time- and space-resolved estimates of the DMS sea surface distribution in this region. Previously developed models for the prediction of marine DMS are on a global scale and do not well represent the Southern Ocean. There is therefore a growing interest in having an algorithm optimized for the Southern Ocean. In this work a satellite-based algorithm was developed, based on ocean chlorophyll concentration (Chl) and sea surface temperature (SST) to predict the sea surface DMS concentration. The model is separated into two temperature regimes, SST below 4^{o}C and SST above 4^{o}C, both corresponding to a different relationship between Chl, SST and DMS. The overall model explained 67% of DMS variance in the Southern Ocean. DMS distribution maps were made using the developed algorithm to predict sea surface DMS concentration from satellite Chl and SST data. High DMS concentrations are observed between latitudes of 40^{o}S and 50^{o}S, and between 60^{o}S to 70^{o}S, with a band of lower DMS in the middle from 50^{o}S to 60^{o}S. Mean latitudinal DMS concentrations for the austral summer period are comparable to previous climatologies, however the predictions for the austral winter period are less reliable due to lack of data. The development of this algorithm can support further studies of DMS-climate interactions in the Southern Ocean.

Key words:

Southern Ocean, dimethylsulphide, phytoplankton, climatology, remote sensing

Contents

List of figures

1. Introduction

1.1 What is DMS?

Dimethyl sulphide (DMS) is a volatile organic sulphur compound with the chemical formula $(CH_3)_2S$. DMS gas is produced biologically in the sunlit layer of the ocean, and is released into the atmosphere, where it plays an important role in the formation of clouds by providing cloud condensation nuclei (CNN).

DMS is the most abundant marine biogenic sulphur compound emitted into the atmosphere, with an estimated flux of 28 Tg S yr^{-1} (Lana, et al., 2011), constituting approximately 70% of the global natural sulphur atmospheric emissions and a major portion of marine organic volatiles emissions (Carpenter et al., 2012).

In the oceans, DMS derives from its precursor dimethyl sulphoniopropionate (DMSP), which is produced by marine phytoplankton. DMSP is believed to fulfil important physiological functions in the phytoplankton cells, these include suggested roles as a cellular cryoprotectant, osmolyte and as an antioxidant under certain environmental conditions (Jarníková & Tortell, 2016; Stefels et al., 2007).

The release of DMSP from the phytoplankton cells can occur through zooplankton grazing, viral attack and phytoplankton autolysis which all result in the breakage of the phytoplankton cells. Once released, the DMSP can be catalysed to DMS via enzymatic cleavage by DMSP lyases, which are enzymes produced by some phytoplankton (Alcolombri et al., 2015) and bacteria (Curson et al., 2011).

Only a small portion of the DMS produced in the seawater is actually released to the atmosphere, through turbulent diffusion. The majority of the DMS is consumed by bacterial oxidation and UV-driven photolysis (Galí & Simó, 2015). Figure 1 shows the process of DMS production from DMSP in seawater.

1.2 Importance of DMS

When released into the atmosphere, DMS is rapidly photo-oxidized to form methanesulphonic acid (CH_3SO_3H), and sulphuric acid (H_2SO_4), which contribute to the formation or growth of aerosol particles (Lana et al., 2011). These aerosol particles allow water vapor to condense around them, thereby acting as cloud condensation nuclei (CCN).

Cloud condensation nuclei are crucial for the formation of clouds. Since in the atmosphere the kinetics of homogeneous nucleation of water molecules is too slow, it is not favourable for the formation of water droplets. To form a small droplet consisting of about 100 water molecules, the humidity of the atmosphere would have to be greater than 200% (Flossmann and Laj, 1998). Therefore, cloud droplets can only form through heterogeneous nucleation when CCN particles are present in the atmosphere.

Through the growth of cloud droplets and the formation of clouds, the atmospheric albedo is altered. The clouds increase the atmospheric albedo by reflecting the incoming solar radiation and impeding it from reaching the Earth's surface. Clouds therefore play an important role in climate and temperature regulation of the Earth.

The individual aerosol particles also enhance light scattering, further increasing the albedo of the atmosphere (Andreae & Rosenfeld, 2008). The DMS derived aerosols are therefore said to regulate cloud micro-physics and atmospheric optics (Andreae & Rosenfeld, 2008). Hence the large amount of marine DMS released into the atmosphere could have a significant impact on the Earth's cloud cover and atmospheric albedo. The atmospheric albedo is influenced by the number of aerosol particles, rather than their mass, since small particles scatter light more efficiently than large particles, and cloud reflectivity is proportional to the number density of cloud droplets.

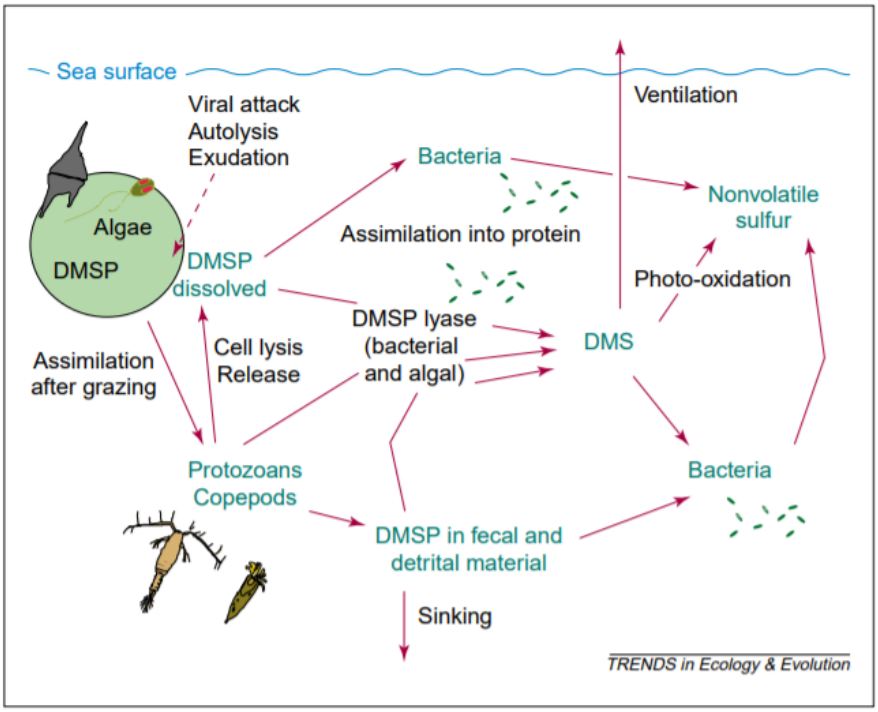

Figure 1 - Illustration of the fate of DMSP in sea water. Source: Simó, 2001.

1.3 DMS and the radiative balance of the atmosphere

Through altering atmospheric albedo, DMS derived aerosol particles can influence the Earth's radiation balance, the balance between incoming and outgoing energy at the top of the atmosphere. This is the total energy available to influence the climate. Energy comes in to the system through solar radiation, and energy can leave the system in two possible ways: reflection (by clouds, aerosols, or the surface of the Earth), and through thermal radiation. The average global net radiation over the period of one year should be around zero to for planet's temperature to remain constant.

Any perturbation in the radiative energy balance is known as a radiative forcing. A perturbation can be caused for example by a change in the concentration of greenhouse gases in the atmosphere, changes in solar radiation or changes in reflective surfaces, such as cloud albedo. These radiative forcings can change the Earth's radiative balance, and have the potential to produce alterations in climate parameters, leading to a new equilibrium state of the climate system.

Such an imbalance is currently being experienced by the impact of increased concentration of greenhouse gases in the atmosphere during recent decades, leading to the global warming of the planet. This effect is known as a positive forcing, in which a climatic factor contributes to the warming of Earth's surface. In contrast, a negative forcing refers to a climate factor which leads to the cooling of the Earth's surface. The DMS derived aerosols in the atmosphere would exert a negative forcing on the climate system.

The negative forcing of the DMS derived aerosols occurs through both direct (reflection of solar radiation by aerosol scattering and absorption processes) and indirect (reflection of solar radiation due to cloud formation) effects (Bopp et al, 2003). Globally, the indirect radiative effect of DMS-derived aerosols is greater than the direct radiative effect.

1.4 The CLAW hypothesis

This role of DMS in climate regulation was first hypothesised in 1987 by Charlson et al. known as the CLAW hypothesis, an acronym named after the authors of the article. They postulated the existence of a negative feedback loop that operates between marine DMS producing phytoplankton and the Earth's climate. In particular, that marine phytoplankton regulate their DMS production in response to changes in the climate, specifically temperature and light conditions, in order to maintain favourable growth conditions.

An increase in available energy, through either increased solar irradiance or a rise in environmental temperature, will result in an increased growth rate of the phytoplankton. An enhanced growth rate leads to an increased production of DMSP and consequently also increases the production of DMS in the seawater. More DMS in the seawater means more DMS will be vented into the atmosphere, increasing the number density of CCN. This in turn elevates the droplet density of the clouds and increases cloud area, leading to greater reflection of solar radiation. This increase in atmospheric albedo in turn protects the phytoplankton from solar radiation as well as excessive temperatures. In this way, an increase in marine DMS flux to the atmosphere could potentially counteract increases in climate forcings, such as greenhouse gases (Vogt & Liss, 2009).

This feedback loop could also perform in reverse, such that a reduction in available energy leads to reduced growth rate of the phytoplankton, causing a decrease in cloud cover, which ultimately allows an increasing amount of solar radiation to reach the surface of the Earth.

The phytoplankton could therefore potentially regulate the climate through the production of DMS. The global potential of this climate feedback loop is still under discussion (Quinn & Bates, 2011), however on regional scales it is evident that marine DMS emissions can have a significant

influence of atmospheric radiative balances (Bopp et al., 2003, Thomas et al., 2010). The feedback system between phytoplankton and climate is shown in figure 2.

The influence of solar radiation on DMS production cycles has already been identified. This evidently shows that there exists a positive correlation between solar radiation and sea surface DMS concentration, in most of the surface ocean, across latitudes and seasons, revealing evidence in favour of the CLAW hypothesis (Vallina and Simó, 2007).

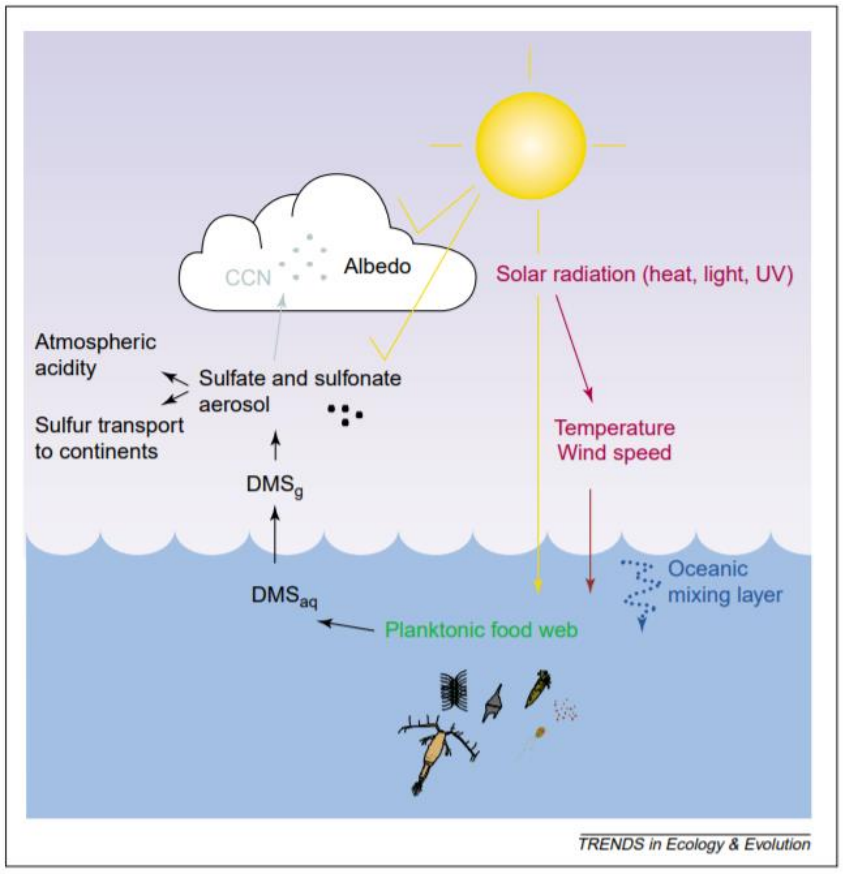

Figure 2 - Illustration of the feedback system between marine phytoplankton and climate, through the production of DMS. Source: Simó, 2001.

1.5 DMS in the ocean

The concentration of DMS in the oceans varies over the seasonal cycle, with maximal concentrations during the summer in high latitudes. At latitudes between 40°N and 40°S, a smaller spring maximum occurs and a larger summer maximum (Vogt & Liss, 2009). Normal DMS concentrations in the ocean are between 1 and 10 nmol L^{-1}, however concentrations up to 300 nM can occur (Simó, 2001).

The DMS concentration in the seawater depends mainly on marine biological productivity and the relative abundance of phytoplankton species. (Bopp et al, 2003). Climate variables such as solar irradiance, sea temperature and ocean physics also affect the DMS concentration, through their influence on the marine biology. (Bopp et al, 2003)

Since bacteria are a main sink for DMS and are involved in the production of DMS from DMSP, as shown is figure 1, factors which affect bacterial activity and taxonomy, therefore also play a role in the regulating the concentration of DMS in the sea. These factors include UV-B radiation, nutrients and dissolved organic matter quality (Simó, 2001).

The flux of the DMS to the atmosphere is controlled by the concentration of DMS at the sea surface and by the magnitude of the DMS transfer velocity across the sea-air boundary. The sea surface is considered to be the upper meter of the ocean. The DMS transfer velocity varies primarily with sea surface temperature (SST) and wind velocity (Wanninkhof, 1992).

Above the ocean, the impact of cloud cover is more significant than above land, due to the lower albedo of the dark ocean surface, leading it to absorb more heat. Also, since the oceanic atmosphere is cleaner, containing less particles than the atmosphere above land, the influence of DMS is much greater in the oceanic atmosphere. Consequently, in the southern hemisphere the predicted effects of DMS derived aerosols on the climate are more important than in the Northern hemisphere (Vogt & Liss, 2009). This adds to the fact that the Southern Ocean is known to be a dominant source of DMS emissions to the atmosphere (Jarníková & Tortell, 2016). Bedsides, the Southern Ocean has more cloud cover than the global average, but most climate models underestimate it and therefore overestimate surface solar radiation and temperature. The origin of these model biases seems to be in an incorrect representation of aerosol-cloud interactions (Bodas-Salcedo et al., 2014)

1.6 The Southern Ocean

The Southern Ocean surrounds the continent of Antarctica, generally defined to be the ocean south of 35^{o}S. The Southern Ocean is unique to other oceans due to the lack of continental obstructions, therefore allowing a current to flow continuously around Antarctica. This current is known as the Antarctic Circumpolar Current (ACC), and the largest current on the planet, and connects all ocean basins. The ACC circles the Antarctic continent from west to east along a path of about 25,000 km, driven by strong westerly winds (Rintoul & Garabato, 2013). These strong winds result in the Southern Ocean being the stormiest and fiercest ocean of the planet (Hanley et al., 2010).

The Southern Ocean has an important role in the climate of the Earth, strongly mitigating the global surface warming. It is estimated that the Southern Ocean south of 30^{o}S, containing 30% of global surface ocean area, accounts for about 43% of anthropogenic CO_2 uptake and around 75% of excess heat uptake of the global oceans (Frölicher et al., 2014).

The transition between the warm subtropical waters and the colder Antarctic water in the Southern Ocean does not occur smoothly, rather there are several sudden transition zones, known as fronts. Apart from sea surface temperature, salinity, oxygen and nutrients also show sudden transitions at these fronts, whereas between the fronts the water properties remain comparatively homogeneous. These fronts therefore define boundaries between waters with distinct environmental characteristics (Orsi et al., 1995).

Traditionally three fronts were defined: Subantarctic Front (SAF), the Polar Front (PF) and the Southern ACC Front (sACCF) (Orsi et al., 1995). In addition to these fronts, there are two more fronts which can be considered; the Subtropical Front (STF) to the north, and the Southern Boundary Front (sBdy) closest to the Antarctic continent, which can be regarded as the northern and southern boundaries of the ACC (Carter, et al., 2008). Figure 3 shows the location of these fronts in the Southern Ocean, however these locations are only approximate since the fronts are dynamic and show year-to-year meridional fluctuations (Kim & Orsi, 2014).

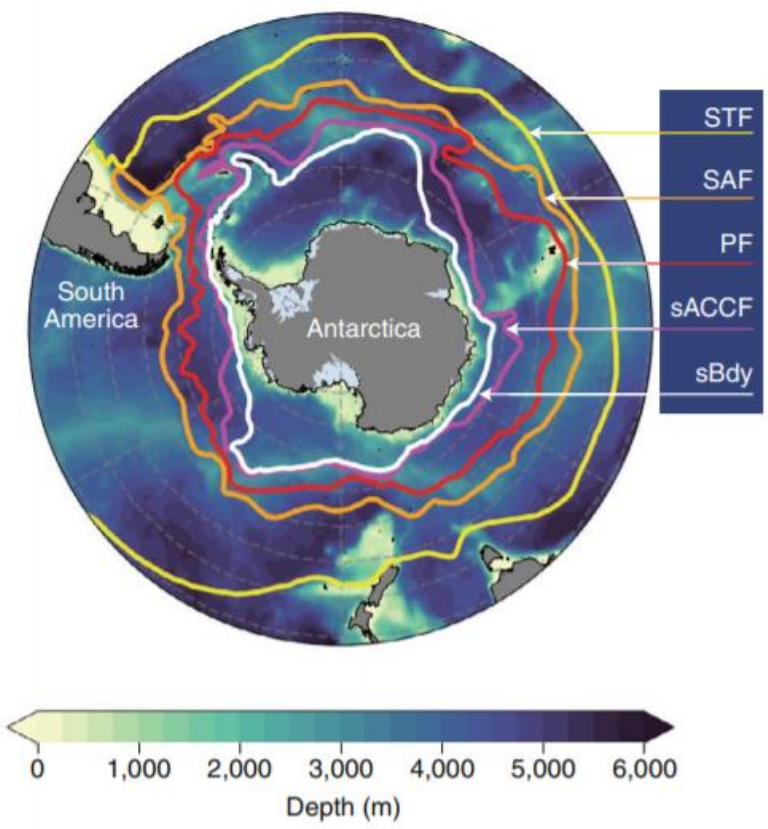

Figure 3 - The circumpolar fronts determined by Orsi et al. (1995). From north to South the named fronts are, the Subtropical Front (STF); the Subantarctic Front (SAF); the Polar Front (PF); the southern ACC Front (sACCF); and the Southern Boundary (SBdy) front. Source: Chapman et al., 2020.

The banded structure of the ACC due to these fronts is the dominant control on biogeochemical distributions in the Southern Ocean, and has an important role in the distribution of nutrients.

A large upwelling of deep ocean water occurs in the ACC, between latitudes of 40^{o}S and 70^{o}S, as shown in figure 4, providing the surface waters with vital nutrients such as nitrate, phosphate, and silicate (Marinov et al., 2006). However, due to limited iron availability in this region the utilization of these nutrients is incomplete. This iron deficiency in the Southern Ocean results in a region known as a 'high-nutrient, low-chlorophyll' zone (Bristow et al., 2017).

Closer to the continental shelves, phytoplankton concentration can reach higher levels. In these shallower waters, the circumpolar fronts interact with the bathymetry which brings iron, derived from sediments, to the surface, leading to the occurrence of phytoplankton blooms (Sokolov & Rintoul, 2007).

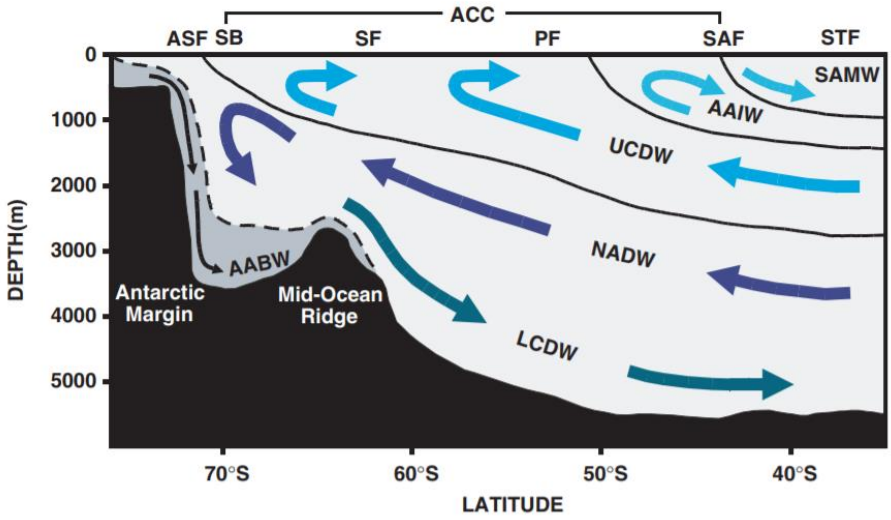

Figure 4 - Schematic section of the main water masses in the Southern Ocean and their meridional transport. Water masses are SAMW, Subantarctic Mode Water; AAIW, Antarctic Intermediate Water; UCDW, Upper Circumpolar Deep Water; LCDW, Lower Circumpolar Deep Water; NADW, North Atlantic Deep Water; AABW, Antarctic Bottom Water. Source: Carter et al., 2008.

1.7 Importance of DMS modelling in the Southern Ocean

It is clear that aerosols and clouds have a significant role in the radiative balance and climate of the Earth. The impact of anthropogenic greenhouse gas emissions on the radiative balance is already well understood, having an estimated average global warming effect of 2.3 W m^{-2} since the beginning of the industrial period (IPCC, 2014). Through the scattering of short-wave radiation as well as increasing the albedo, lifetime, and cover of clouds, aerosols both anthropogenic and natural counteract this warming effect by about −0.9 W m^{-2} (IPCC, 2014).

The radiative effect of natural aerosols, however is less well understood, constituting to the major uncertainty in estimations of aerosol radiative effects and their impact on climate (Carslaw et al., 2013). Therefore, an improved understanding of these natural aerosol sources, such as DMS, is needed. By estimating the distribution of DMS with sufficient spatial and temporal resolution, the impact it has on the climate could be better studied.

The Southern Ocean is the region of the Earth where the marine DMS emissions are expected to have the greatest effect on the climate (Thomas et al., 2010). The extent of this effect however, cannot be well quantified currently, due to the lack of a model which represents well this region of the ocean. This leads to a growing interest in having a satellite algorithm optimized for the Southern Ocean.

Compared to many other oceanic regions, the Southern Ocean is relatively data-sparse. This lack of data is largely due to the remoteness and harsh climate of the Southern Ocean, which puts significant logistical constraints on the operation of research ships in these polar waters. During the winter season a large area of the Southern Ocean is covered by sea ice which makes exploration of the waters near impossible, therefore sampled data is mainly obtained during summer months.

Recently more data measurements are being gathered for the Southern Ocean, and have been added to the global DMS database started by Kettle et al. (1999). This database has been a major milestone in DMS research. This data will be used to develop a satellite-based algorithm to predict the DMS concentration in the sea surface of the Southern Ocean.

1.8 Previous models

Previously developed models to predict the sea surface concentrations of DMS consist of both prognostic and diagnostic approaches. The diagnostic models use empirical relationships between DMS and environmental variables, whilst the prognostic models account for the processes controlling the sinks, sources and cycling of DMS. Although the prognostic models are more complex than the diagnostic models, they do not necessarily show an improvement in reproducing observations.

Table 1 gives a summary of the currently available models for DMS predictions. Most of these models have been developed for the global ocean. There is a wide variety of input fields used between the different empirical models. The majority of the models use chlorophyll as a main predictor variable. Other commonly used variables are the mixed layer depth (MLD), and variables related to light, such as the daily-averaged solar radiation dose (SRD). The most recently developed empirical model, by Galí et al. (2018), expands to using a larger number of input variables, including sea surface temperature (SST), euphotic layer depth (Zeu), particulate inorganic carbon (PIC) and photosynthetically available radiation at the sea surface (PAR).

A comparison of the models listed in table 1 (except Galí et al., which was developed later), was carried out by Tesdal et al. (2015). Their study tested the climatologies, empirical and prognostic models of DMS concentration in the surface ocean against each other and against observations. They conclude that none of the currently available models for estimating the global surface ocean DMS distribution reproduced the observed DMS concentration in the ocean very well. The various empirical models show very different spatial patterns, of which none correlate strongly with observations. Both the empirical and prognostic models generally tend to underestimate the DMS concentration compared with the best available data-based estimates.

Even though the global DMS models do not show a very promising result so far, earlier studies suggested that linking DMS to key parameters is possible on a smaller regional scale for a specific period of the year (Aranami &Tsunogai, 2004; Miles et al., 2012; Kameyama et al., 2013). This is due to different ocean regions having unique environmental and oceanographic characteristics.

For this reason, the current global models have likely not performed well in the Southern Ocean region. Since presently there does not exist a model specifically for the Southern Ocean, this

work aims to develop an empirical model for the estimation of DMS uniquely tuned to this region.

Table 1. Basic characteristics all currently available DMS climatologies and models.

Name	**Reference**	**Input fields**	**Region**
K99	Kettle et al., 1999	Climatology	Global
K00	Kettle & Andreae, 2000	Climatology	Global
L10	Lana et al., 2011	Climatology	Global
AN01	Anderson et al., 2001	Chlorophyll, nitrate, surface irradiance	Global
AU02	Aumont et al, 2002	Chlorophyll, silica	Global
SD02	Simó & Dach, 2002	Chlorophyll, MLD	Global
AT04	Aranami & Tsunogai, 2004	Chlorophyll, MLD	North Pacific
BE04	Belviso et al., 2004	Chlorophyll	Global
VS07	Vallina and Simó, 2007	MLD, SRD	Global
MI09	Miles et al., 2009	MLD, SRD	Atlantic
HadOCC	Collins et al., 2011	Chlorophyll, MLD	Global
G18	Galí et al., 2018	Chlorophyll, MLD, SST, Zeu, PIC, PAR	Global
HAMOCC	Kloster et al., 2006; Six & Maier-Reimer, 2006	Prognostic	Global
PlankTOM	Vogt et al.,2010	Prognostic	Global
PISCES	Belviso et al., 2012	Prognostic	Global
POP-TGM	Elliott, 2009	Prognostic	Global

2. Aims and objectives

Aim:

To develop a satellite-based algorithm to calculate the concentration of DMS in the sea surface water of the Southern Ocean.

Objectives:

- Compile a data set of in situ DMS measurements, obtained from a public DMS database, and unpublished data from supervisors and other collaborators, and perform quality control.

- Complement the dataset with corresponding satellite measurements of chlorophyll, irradiance, temperature, water transparency, etc.

- Analyse the ability of existing global algorithms to capture the variability of the observations. Adjust them and/or design a new regional algorithm if necessary.

- Produce monthly maps of sea surface DMS concentration in the Southern Ocean.

- Interpret the results and discuss their biogeochemical and climatic implications

3. Methods

3.1 Data

Measurements of in situ DMS concentration (DMS_is, nmol L^{-1}), along with surface sea temperature (SST, ^{o}C) and salinity were obtained from the global sea-surface (GSS) DMS database (https://saga.pmel.noaa.gov/dms/). Since this work focuses on the Southern Ocean, only latitudes south of -35^{o} were considered. This GSS dataset offered data from the years 1990 to 2017. DMS measurements from three additional cruises in the Southern Ocean, not currently present in the GSS database, were added to the dataset; ACE, Pegaso and TransPegaso. All DMS measurements where the sea salinity was below 30 were removed since these correspond to waters with very strong influence from ice melting.

In situ DMS measurements are classically done through gas chromatography, requiring a preconcentration of gas, using a purge and trap technique. As this method is carried out manually, it only allows for a limited number of measurements per day. Since 2005 continuous DMS in situ measurements have been possible (Tortell, P.D., 2005; Kameyama et al., 2009; Saltzman et al., 2009), offering a much greater number of daily measurements. To give a more even weight is given to different data measurements, the data was binned.

The binning of the GSS dataset reduces the size of the dataset whilst retaining the information. This binning was achieved by grouping the in situ data by date, latitude, longitude and contribution number (number assigned to each cruise which contributed in situ DMS measurements). Temporally the binning was done on a daily period. Spatially the binning was done using a grid with 4.9km resolution in both the latitudinal and longitudinal directions. This grid, called sinusoidal equal-area grid, is appropriate for polar areas because all pixels have the same area. The mean value of in situ DMS was calculated for each grouping, or bin. This resulted in a binned dataset of 10291 rows, compared to the original 21709 rows of unbinned data.

Remotely sensed satellite data of the ocean was matched up against the binned in situ DMS dataset. The matchup data corresponds to satellite observations that are closest in space and time to a given in situ measurement. These satellite matchups include the following variables; chlorophyll a (Chl, mg m^{-3}), euphotic Layer Depth (Zeu, m), vertical attenuation coefficient at 490 nm (K_{d490}, m^{-1}), particulate inorganic carbon (PIC, mol m^{-3}) and daily photosynthetically available radiation at the sea surface (PAR, mol photons m^{-2} d^{-1}). The satellite data matchups were done against position (latitude and longitude), and the date of each in situ DMS measurement. Approximately 10% of the binned dataset had matchup satellite data available.

The matchup data was downloaded from the European Space Agency's GlobColour project (https://www.globcolour.info). The data for the matchups were taken from four different satellite sensors, to maximize the number of observations available. The details of each satellite sensor are given in table 2. These sensors observe the spatial and temporal distribution of phytoplankton chlorophyll in the sea surface. The concentration of chlorophyll is derived from the ocean reflectance spectrum in the visible range. The standard chlorophyll measurement is determined through the colour tone of the sea surface, defined by the blue/green ratio, such

that a green colour indicates a high chlorophyll concentration whilst a blue colour signifies a lower chlorophyll concentration. The GSM chlorophyll algorithm additionally takes into account the light absorption by other seawater constituents, which improves chlorophyll values in coastal waters. GSM chlorophyll refers to chlorophyll measurements calculated using of the Garver-Siegel-Maritorena model (Maritorena & Siegel, 2005).

Table 2 – Details of the satellite sensors used for matchup data. Source: https://www.globcolour.info

Sensor	Resolution	Start Date	End Date	Reprocessing Version
SeaWIFS	4km	1997-09-04	2010-12-11	NASA R2018.0
MODIS-Aqua	1km	2002-07-03	Present	NASA R2018.0
VIIRS SNPP	1km	2012-01-02	Present	NASA R2018.0
VIIRS JPSS-1	1km	2017-11-29	Present	NASA R2018.0

As seen in table 2 the earliest date for which satellite data is available is in 1997, therefore regardless of the global sea-surface DMS database having data since 1990, only data for which satellite matchups are available was used.

Bathymetry (BD, m) and mixed layer depth (MLD, m) were also matched up against the dataset. These are both non satellite measurements and were obtained from the following sources; the 0.5^{o} resolution bathymetry matchups were obtained from the General Bathymetric Chart of the Ocean (https://www.gebco.net/), and the 0.5^{o} resolution MLD matchups were obtained from NOAA (https://www.pmel.noaa.gov/mimoc/#netCDF).

The final dataset contained data from 1997 to 2017, covering the months from October to May Figure 5 and figures 6a and b, show the spatial and temporal and distribution of the DMS in situ measurements used for the development of the algorithm.

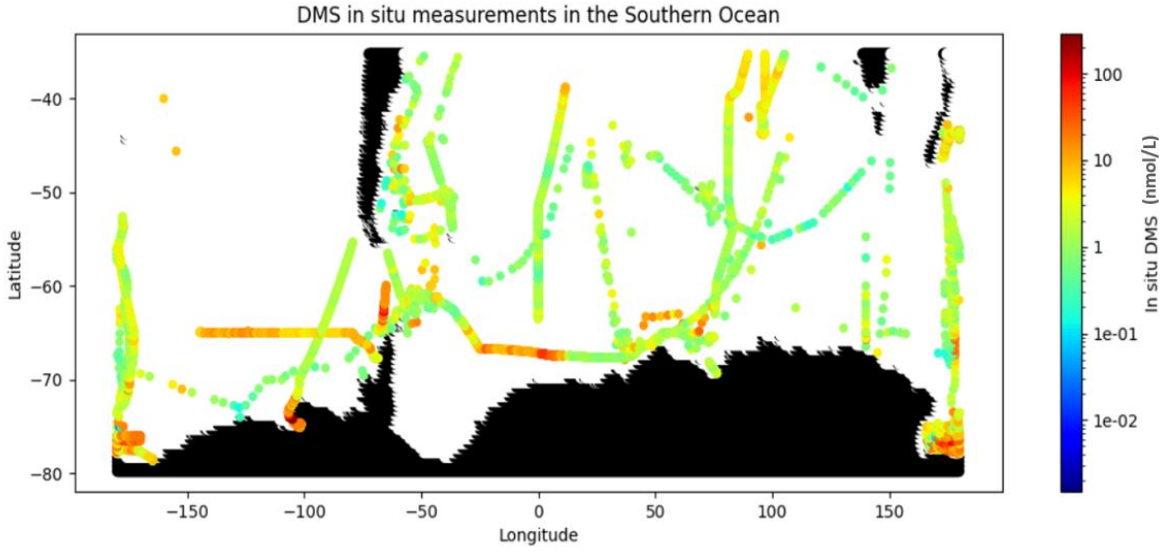

Figure 5 - Spatial distribution of in situ DMS measurements in the Southern Ocean.

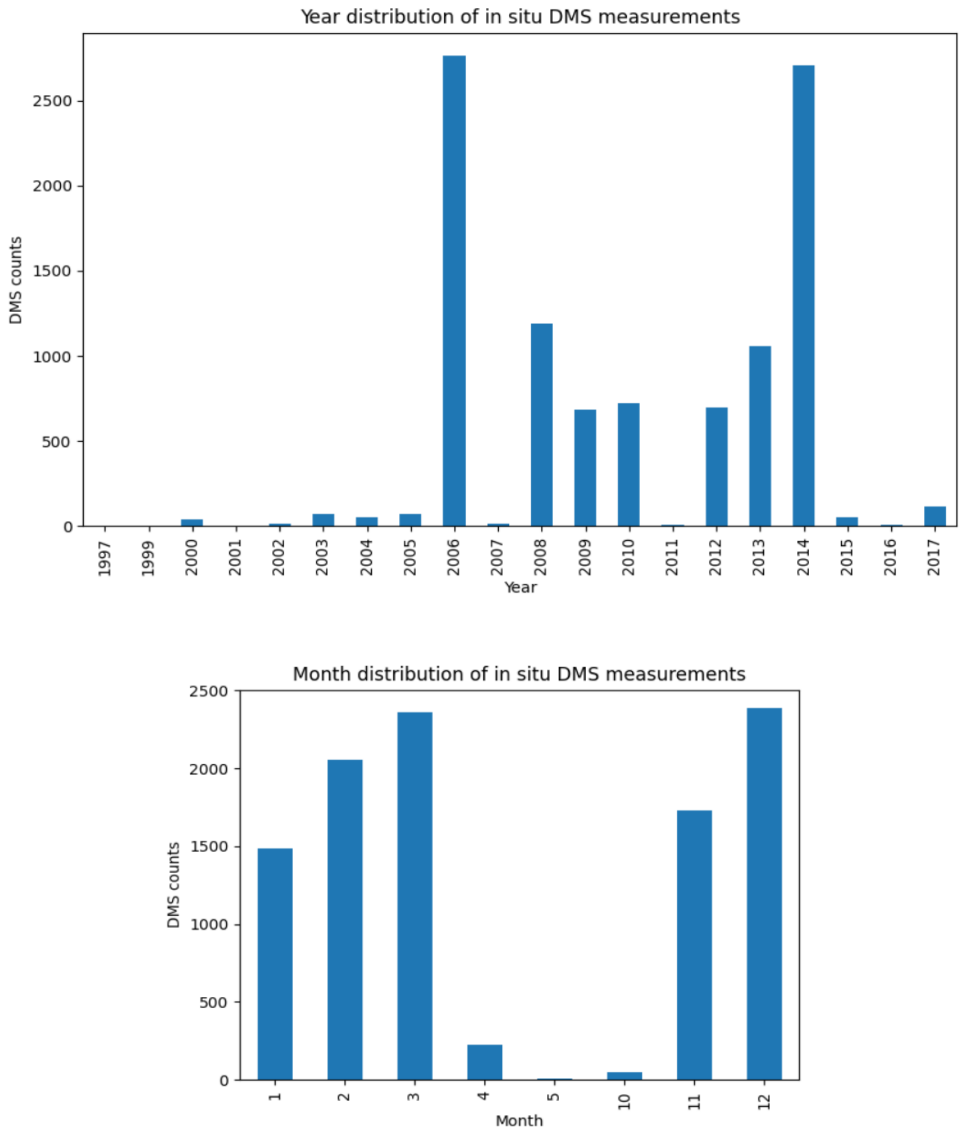

Figure 6 - Temporal distribution of in situ DMS measurements, a) yearly distribution (top) and, b) monthly distribution (bottom).

3.2 Statistical analysis

Since previous models for the prediction of marine DMS did not perform well in the region of the Southern Ocean, new statistical relationships were developed. The variables explored for the prediction of the concentration of DMS were the most common variables used in previous models, namely; Chl, SST, MLD, ZEU, PIC, PAR and solar radiation dose (SRD).

Multiple linear regression analysis was carried out to understand the relationship between these predictor variables and the criterion variable, being in situ DMS. The criterion variable was modelled as a function of the predictor variables, and the coefficient of determination (R^2) of the relationship and the coefficients of the variables were used to determine the significance of each predictor. The rR^2 value provides the proportion of the variance in the criterion variable

that is predictable from the predictor variables, whereby a value closer to 1 is more favourable, since it indicates that a larger percentage of variance is covered by the relationship.

The relationship of each single predictor variable against in situ DMS were first analysed. Next all combinations of two predictors were evaluated against DMS, after which all combinations of three predictors, and so on until reaching all the predictors. This allowed to understand the impact of adding predictors to the relationship, through which the simplest relationship which covered the greatest variance could be identified. Predictor variables which did not offer much improvement to the relationship were therefore removed to simplify the model.

Non-linear relationships were also investigated through multiple regression analysis, with the following relationships as predictor variables: Chl/MLD, PAR/MLD, Chl*PAR, 1/Chl, SST^2, Chl^2. The rationale for exploring these nonlinear predictors is that they might be better able to capture phytoplankton growth and physiology. Furthermore, the logarithmic relationships were also explored, specifically between $\log_{10}$(Chl) and $\log_{10}$(DMS). The rationale for applying logarithmic transformation to these variables is the approximate log-normal shape of their frequency distribution.

Different bottom depth limits were also investigated to understand the impact of this variable on the regression relationships. All data points with a bathymetry shallower than 200m were excluded, since such coastal waters do not well represent the behaviour of the open ocean.

3.3 Algorithm development

Once the variables which covered the greatest proportion of variance for the prediction of DMS were identified, a model could be formed for the calculation of DMS from these variables. The model was developed through calculating the least squares regression fit of the variables which covered greatest proportion of variance against the in situ DMS. The equation of this regression line was used as the basis of the model, used to calculate the concentration of DMS.

The application of certain variables filters was experimented in an aim to improve the model. In addition to R^2, the Root Mean Square Error (RMSE), Mean Absolute Percentage Error (MAPE) and Mean Bias Error (MBE) were also calculated to determine accuracy of the model.

To determine the accuracy of the model, linear regression analysis was then performed between the calculated DMS concentration (DMS_calc) and the in situ DMS concentration (DMS_is), to check the similarity between these two values. Ideally the graphical representation of DMS_is against DMS_calc would show the best fit along the 1:1 line, which would indicate perfect prediction, (having an R^2 value of 1) and no error (having an RMSE, MAPE and MBE of 0).

Outlying data points were identified and removed to improve the relationship. In general, data points were considered outliers if they were more than two standard deviations (2σ) from the least squares fit.

The algorithm was defined by the model which provided best least squares regression fit between DMS_calc and DMS_is, with the exclusion of outlying data points.

3.4 Algorithm implementation

Once the algorithm was developed it was used to calculate DMS concentrations in the Southern Ocean. This was calculated using 1/12^{o} resolution monthly climatological data of the variables applied in the model. This data was obtained from Nasa's OceanColor database (https://oceandata.sci.gsfc.nasa.gov/). The data measurements were those from the MODIS-Aqua satellite sensor. Since this sensor came to use in 03/07/2002, the monthly climatology data used was for the period between July 2002 and July 2021.

Matchups of 1/12^{o} resolution bathymetry measurements were added to the monthly climatological dataset to be able to filter out undesired ocean depths, according to the specifics of the developed algorithm.

DMS maps for the Southern Ocean were created for each month, using the predicted DMS concentrations from the developed algorithm, and the seasonal cycle of mean DMS concentration over latitudes was analysed.

The resulting calculation of sea surface DMS concentrations, were compared with the climatology data of Lana et al. (2011) and Kettle et al., (2000).

4. Results

4.1 Statistical analysis

GSM-derived satellite chlorophyll (Chl_GSM) was used to carry out the statistical analysis since it agreed better with in situ chlorophyll measurement, in terms of linear correlation, than the standard satellite chlorophyll (Chl1), (Chl_GSM; R = 0.73 and Chl1; R = 0.71). In addition to Chl_GSM offering a better correlation, it also offered more matchup data points than Chl1, due to fewer pixels being discarded for optical issues.

It was found that there exists a different relationship between Chl_GSM and DMS_is dependent on the temperature, suggesting two separate regimes, one in the cold waters and another in the warmer waters. This division in behaviour was determined to occur at SST of 4^{o}C. Figure 7a shows the relationship between Chl_GMS, SST and DMS_is, and figure 7b shows the difference in the relationship between Chl_GSM and DMS_is for the two identified temperature zones. Due to these two temperature regimes, two different models were developed, for the cold water (SST < 4^{o}C) and for the warm water (SST > 4^{o}C).

From the multiple regression analysis, the variables Chl_GSM and SST always resulted in the highest R^2 values, therefore covering the greatest variance. The addition of some other variables to the relationship, did increase the R^2 value, but by such a small amount that the contribution was considered insignificant.

The non-linear relationships tested showed minimal improvement for the prediction of DMS, and as a result were rejected. The logarithmic relationship of $\log_{10}$(Chl_GSM) and SST as predictor variables and $\log_{10}$(DMS_is) as the criterion resulted in the highest R^2 value from all the tested relationships. Also, the logarithmic relationship was the only relationship that had a sufficiently high R^2 value and did not result in the calculation of negative DMS values. Therefore, the logarithmic relationship was used to further develop the model.

Both temperature regimes could be well represented through the logarithmic relationship between $\log_{10}$(Chl), SST and $\log_{10}$(DMS), however, the behaviour of each temperature zone was represented by a different relationship between the variables.

From the investigation into different bottom depth limits, it was found that the regression relationships could be improved through filtering out all data point belonging to a bottom depth shallower then 1000m, which corresponds to coastal waters. The model was therefore developed for the open ocean, where the bottom depth was deeper than 1000m. Setting the bathymetry boundary to deeper than 1000m did not significantly improve the relationship, hence the limit of 1000m was opted.

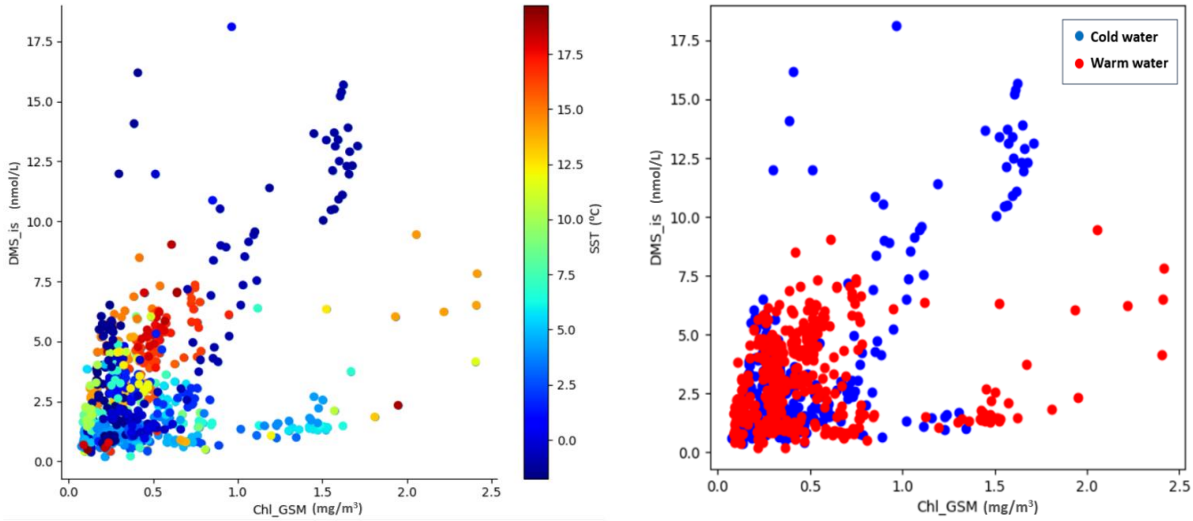

Figure 7 – Shows the two distinct temperature regimes. a) Shows the relationship between Chl_GSM and DMS_is as a function of SST (left). b) Illustrates this relationship by defining data points of the cold water (SST< 4°C) in blue and those of warm water (SST>4°C) in red (right).

4.2 Algorithm development

The model developed for the cold-water regime for the calculation of DMS is the given in equation 1:

$$\log_{10}(\text{DMS}) = 0.64 \log_{10}(\text{Chl\_GSM}) - 0.08\ \text{SST} + 0.661 \qquad \text{(Eq. 1)}$$

This equation allowed for the calculation of DMS_calc where SST is lower than or equal to 4°C. Analysed DMS_calc against DMS_is results in an R^2 value of 0.75 (n = 386). A total of 6 data points were identified as outliers and removed from dataset. Figure 8a shows the relationship between DMS_calc and DMS_is in the cold-water regime. It can be seen that DMS_calc underestimates DMS_is at high concentrations.

In the warm-water regime, investigation revealed that the relationship could be improved by excluding data points where SST is greater than 18°C. An additional 5 datapoints were removed from being further than two standard deviations from the least square fit. The model for the warm water regime is given by equation 2.

$$\log_{10}(\text{DMS}) = 0.111 \log_{10}(\text{Chl\_GSM}) + 0.048\ \text{SST} - 0.074 \qquad \text{(Eq. 2)}$$

Linear regression of the DMS_calc, determined through equation 2, against DMS_is resulted in a R^2 value of 0.608 (n = 399). This relationship of the warm-water regime is shown in figure 8b. As in the cold-water regime, the model for the warm-water regime also underestimates DMS_is at high DMS concentrations.

It can be seen clearly in figure 8b that the warm water relationship is very dependent on temperature, and this dependence is positive, with a general trend to increased DMS at higher SST. Conversely, in cold water the relationship was found to be more dependent on Chl rather than SST, and the SST had a negative effect; DMS increased towards colder SST.

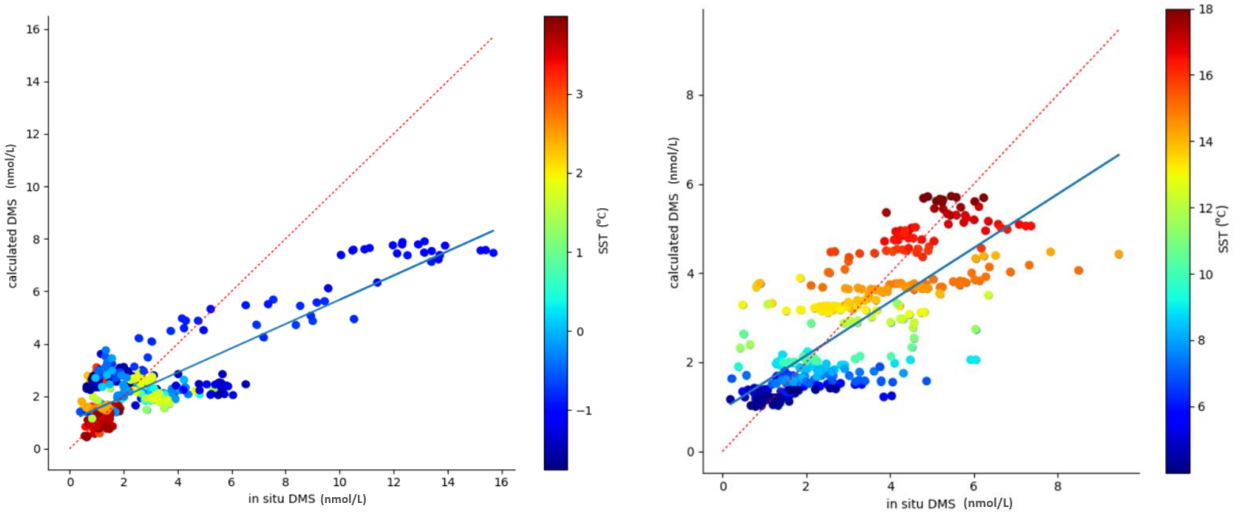

Figure 8 - Plots of DMS_is against DMS_calc for a) The cold-water regime (left) and b) the warm-water regime (right). The blue line indicates the least squares fit and the red line marking the 1:1 line.

Figures 9a and b show the behaviours of equations 1 and 2. In cold water regime, at low SST and low Chl, DMS_calc is also low. With increasing Chl, DMS_calc increases, reaching higher concentrations at low temperatures. In the warm water regime, at low SST and low Chl the DMS_calc concentration also remains low, similar to the cold water behaviour. Again, the DMS_calc increases with increasing Chl concentration, however contrary to the cold-water regime, in the warm-water regime maximum DMS_calc concentrations are achieved at high SST. It can also be seen that the maximum DMS_calc concentrations produced in cold waters are higher than in warm waters.

Combining the two temperature regime models together the DMS can be calculated for the entire Southern Ocean. Figure 10 shows the resulting relationship between DMS_is and DMS_calc for the entire temperature range, resulting in an R^2 value of 0.67 (n = 785).

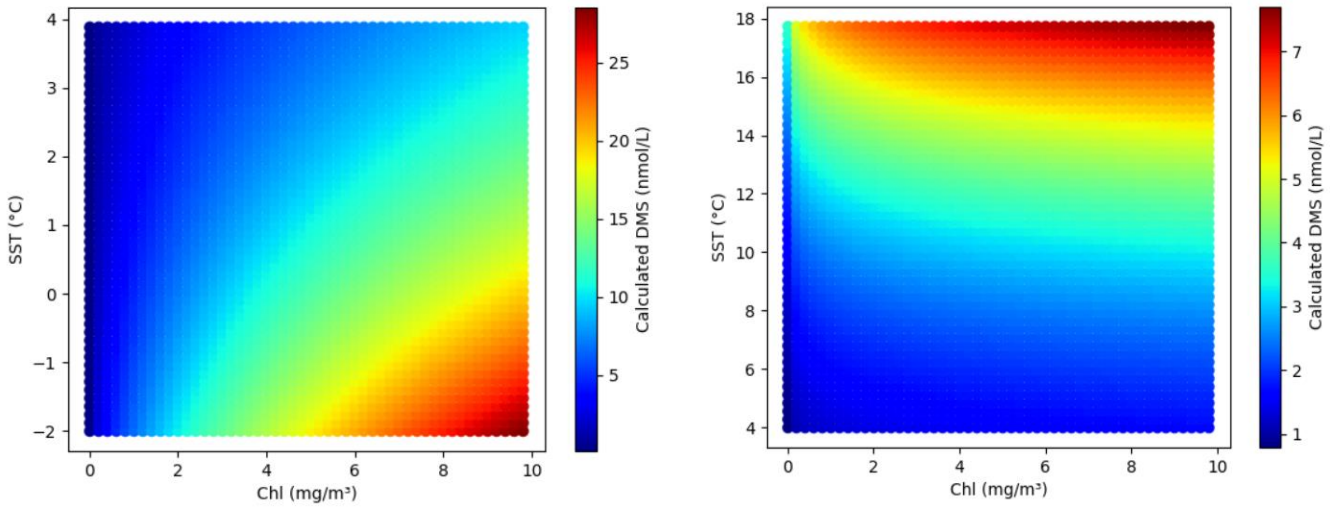

Figure 9 - Visualization of the relationship between Chl, SST and DMS_calc a) in the cold-water regime, represented by equation 1 (left) and, b) in the warm-water regime, represented by equation 2 (right).

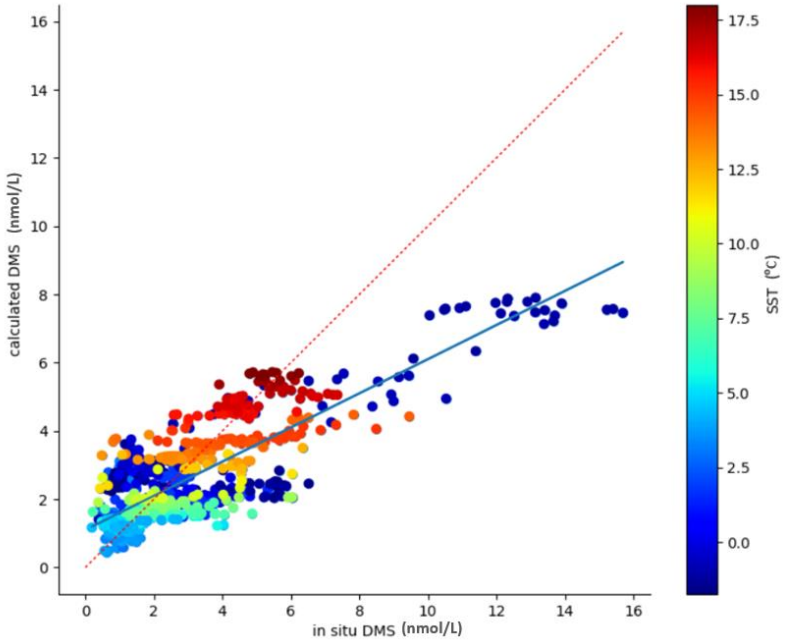

Figure 10 - Plot of DMS_is against DMS_calc for the both temperature regimes combined. The blue line showing the least squares fit and the red line marking the 1:1 line.

Table 3 shows details of the statistics calculated for each model, including Root Mean Square Error (RMSE), Mean Absolute Percentage Error (MAPE) and Mean Bias Error (MBE). The negative mean bias error indicated an underestimation of the model, as was seen in figures 8a and b.

Table 3. Model statistics for the different temperature regimes and both regimes together.

	Cold regime	**Warm regime**	**Both regimes**
n	*386*	*399*	*785*
R^2	0.75	0.61	0.67
RMSE (nmol L^{-1})	1.87	1.129	1.54
MAPE (%)	51.97	37.75	44.75
MBE (nmol L^{-1})	-0.50	-0.22	-0.36

4.3 Algorithm implementation

Figure 11 shows the monthly maps of DMS_calc, produced using satellite climatology data of Chl_GSM and SST. In general, bands of high DMS are seen between 40^{o}S and 50^{o}S, and between 60^{o}S to 70^{o}S, with a band of lower DMS in the middle from 50^{o}S to 60^{o}S.

The highest DMS concentrations are observed at latitudes between 60^{o}S and 70^{o}S, reaching a maximum of 9 nmol L^{-1} in January. In the band between 40^{o}S and 45^{o}S, the maximum DMS concentrations do not reach as high as in the 60^{o}S to 70^{o}S band, with maximum values between 5.6 and 6.5 nmol L^{-1} throughout the year. The highest DMS concentrations predominantly occur in the summer months, from December to March. At low latitudes a peak in DMS occurs in the month of June, which derives from peaks in both mean Chl and mean SST during this month (figures 12b and c). This behaviour cannot be confirmed at lower latitudes due to lack of satellite data, so consequently DMS_calc could not be computed.

At low latitudes of 40^{o}S to 50^{o}S, there is a clear seasonality visible in monthly mean DMS concentration, which peaks in February and March at 2.9 nmol L^{-1}, and minimum mean DMS occurring in the months of August September, at 1.9 nmol L^{-1}, as seen in figure 12a. However, the month of June posed an exception to this seasonality pattern, also having a mean DMS concentration as high as that of February and March. At higher latitudes, lack of data does not allow for a clear relationship to be stated. In the months for which data is available in the high latitudes, peak mean DMS concentrations also occur in the summer, from December to February. In general, the mean DMS concentration in the lower latitudes is greater than in the higher latitudes, with a mean of 1.9 – 2.9 nmol L^{-1} between 40^{o}S and 50^{o}S, and 1 – 1.7 nmol L^{-1} at higher latitudes, with the available data.

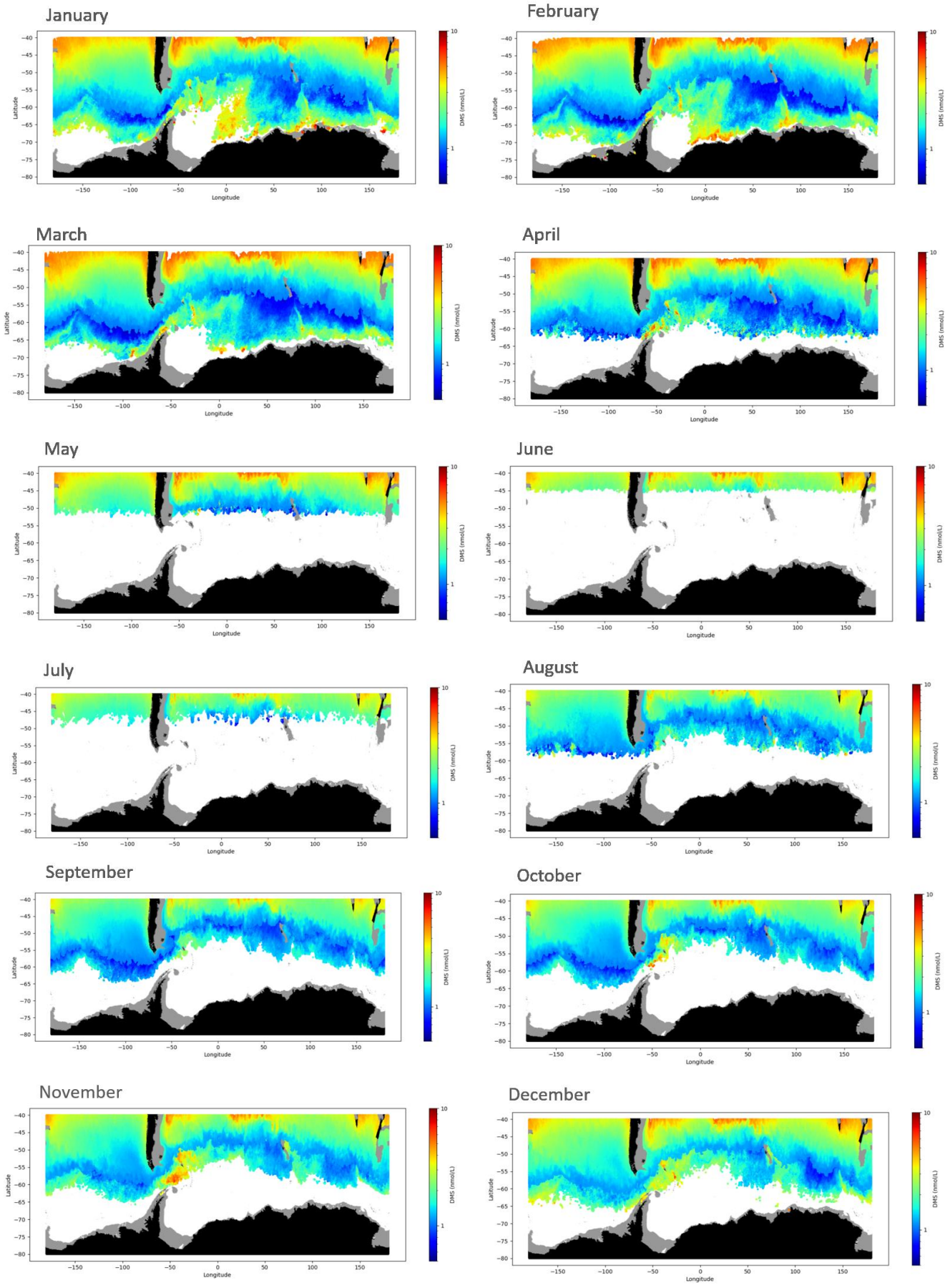

Figure 11 - Monthly maps of calculated DMS distribution in the Southern Ocean.

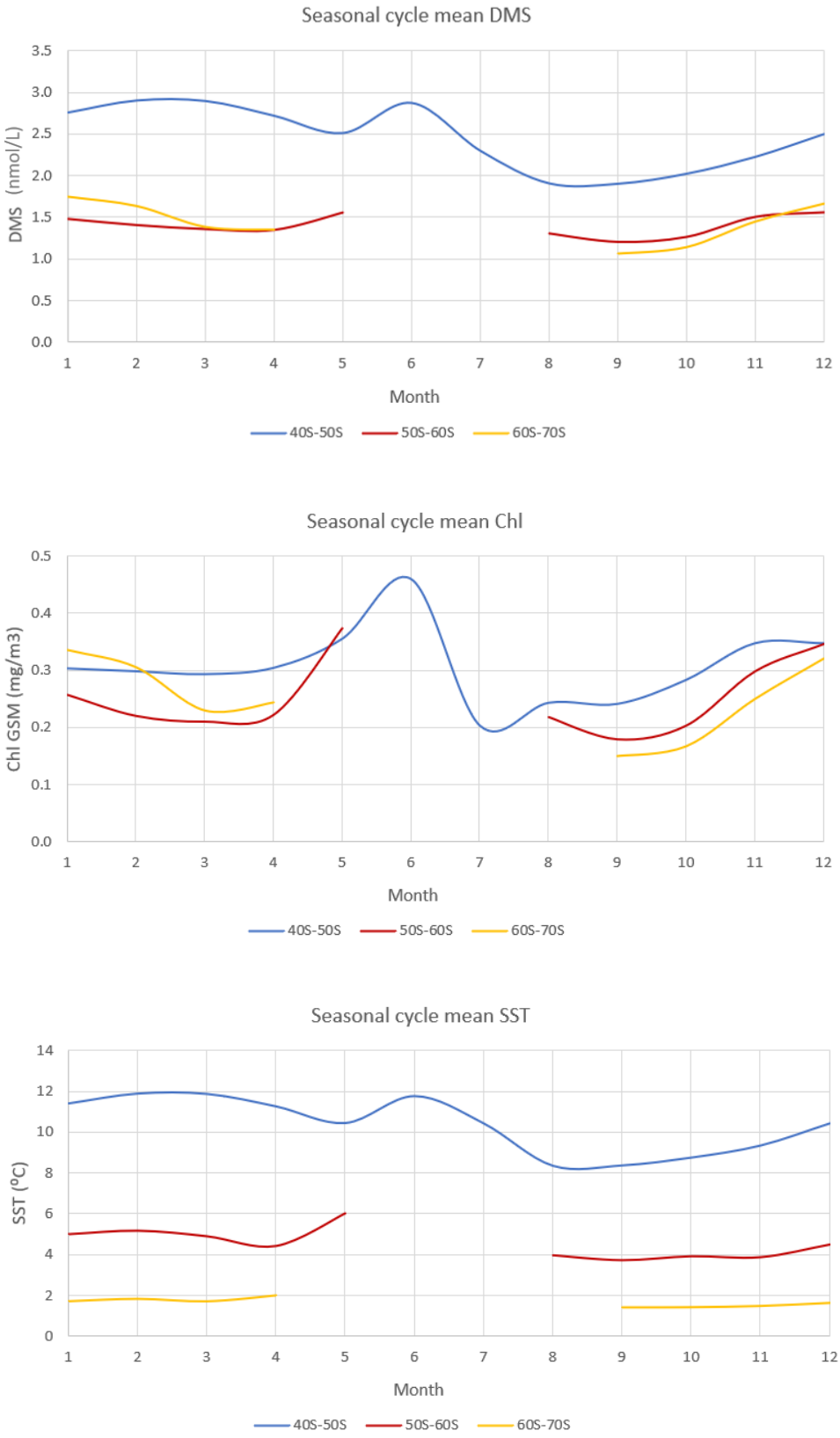

Figure 12 - Seasonal cycles by latitude band of a) mean DMS_calc (top), b) mean Chl_GSM (middle) and c) mean SST (bottom).

The resulting sea surface DMS concentration calculated with the model developed in this work (hereafter referred to as M21), was compared with the climatologies of Lana et al. (referred to as L10), and Kettle & Andreae (referred to as K00). Figures 13a and b show the comparison of annual mean DMS and seasonal mean DMS across the latitudes of the Southern Ocean. The seasonal analysis was done for the austral summer months; December, January and February (DJF) and the austral winter months; June, July and August (JJA). The data plots of K00 and L10 were obtained from Lana et al., 2011, cut to show latitudes of the Southern Ocean only.

As can be seen in figure 13a the annual mean DMS of M21 shows a similar behaviour to that of K00 and L10, especially at low latitudes. At latitudes between 40°S to 50°S M21 shows a higher DMS concentration than the climatologies. Also, in M21 a small peak is observed around 70°S, which does not seem consistent with the rest of the data.

For the comparison of the seasonal mean DMS, shown in figure 13b, M21 shows less correlation to K00 or L10 as with the annual mean DMS. Both the austral summer period (DJF) and the austral winter period (JJA) show slightly different behaviours. In the summer period, M21 shows lower DMS values than K00 and L10 predicted. In the winter period, M21 indicates similar DMS concentrations as compared to the summer period, only slightly lower, however this behaviour is not at all portrayed in K00 or L10, which shows winter DMS concentrations significantly lower than the summer values. In the austral winter, data of M21 is only available until 60°S therefore an accurate comparison across all latitudes cannot be carried out.

The behaviour of the austral summer period in M21 is very much reflected in the annual mean DMS concentrations since these are the months which contain the most data points, making them the most dominant. In general, the behaviour of the summer period is comparable to that of the climatologies, decreasing in DMS concentration from around 40°S to 50/60°S, thereafter increasing rapidly in concentration moving towards 80°S.

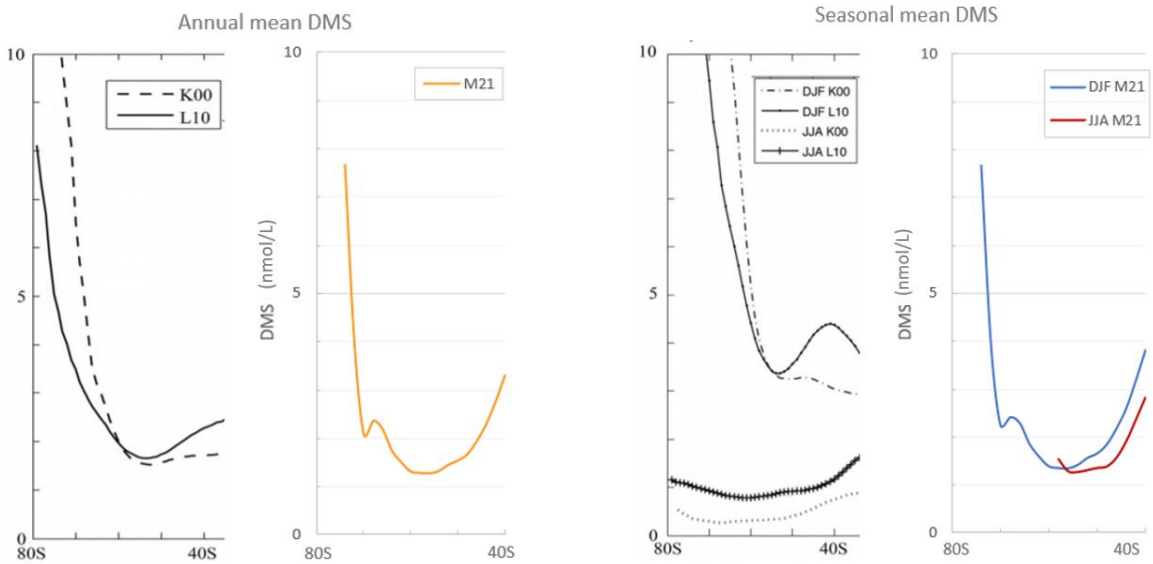

Figure 13 - Comparisons on M21 to climatologies K00 and L10 for a) annual mean DMS (left), and b) seasonal mean DMS (right).

5. Discussion

5.1 Algorithm development

It was opted to use Chl_GSM and SST as the only predictor variables for the algorithm since these are both well tested and well validated satellite variables. It was preferred to use as few variables as possible to keep the model simple, and since the addition of other variables did not add significant improvement to the model, they were not included.

For the development of the model, Chl_GSM satellite data of a temporal resolution of 1 day was used only, since these are the most precise measurements. Using 8-day Chl_GSM data in addition with the 1-day data would have expanded the data set, however making the Chl_GSM data values less accurate.

The algorithm was developed using the in situ SST measurements rather than the satellite measurements, however the in situ and satellite measurements of SST correspond well., previous analysis of the global-scale SST in situ GSS data against satellite SST matchups by Galí et al. (2015), yielded an R^2 value of 0.99 and RMSE value 0.8^{o}C. Therefore, the satellite measurement of SST can equally be used in the algorithm.

The model excluded datapoints from a water column depth shallower than 1000m since this corresponds to shelf and coastal waters, which have distinct biogeochemical and optical characteristics that make them behave differently from the open ocean (Ardyna et al., 2017). The developed algorithm therefore only applies the open ocean, at depths greater than 1000m.

This work shows how the behaviour of DMS is dependent on the region of the ocean. Even looking only at the Southern Ocean, two distinct behaviours between chlorophyll and DMS were already be detected, with an SST boundary determined at 4^{o}C. A similar temperature boundary was found by Rodríguez-Ros et al. (2020) when exploring the pattern of isoprene distribution in the Southern Ocean. They found an SST boundary at 3.4^{o}C, when investigating chlorophyll to isoprene relationships. Similarly, Ooki et al. (2015) had also found such a temperature boundary prior for the relationship between chlorophyll and isoprene in the Southern Ocean, their temperature boundary was determined at 3.3^{o}C. These boundaries coinciding around 3-4^{o}C roughly correspond to the southern boundary of the Polar Front, which is known to separate chemical and biological regimes.

In the warm-water regime, the removal of datapoints where SST was greater than 18^{o}C significantly improved the model fit. This could be due to the 18^{o}C boundary corresponding to the boundary of the Subtropical Front, which may result in a region with different biogeochemical characteristics.

It must be stressed that the algorithm developed in this work calculates the DMS concentration in the surface of the ocean, not the DMS emitted into the atmosphere. To know the DMS flux to the atmosphere further calculation is needed, for which models already exist (Kettle & Andreae, 2000; McGillis et al., 2000).

5.2 Algorithm implementation

Monthly climatology data for the calculation of the DMS maps were only available for Chl_GSM, not for SST. To recreate climatology data for SST, the monthly mean values of SST were calculated between the years 2003 and 2020. Also, for unknown reasons, monthly climatology data for the month of July was not available from the NASA OceanColor website, therefore to obtain the data for this month the same process as with the SST was performed, calculating the mean Chl value from July 2003 and July 2020 monthly data.

For the DMS maps it was opted to remove data north of 40^{o}S, due to reduced reliability of DMS_calc predicted in this area. In addition, datapoints for which satellite measurements of Chl were above 2.5 mg m^{-3} were removed since these are considered abnormally high values. The data used for the algorithm development did not contain Chl values greater than 2.5 mg m^{-3}, and it is not recommended to extrapolate algorithms too far from the range of observations used for the development.

It can be seen in the DMS maps in figure 11 that the pixels at the southern border of the observable area look patchy because of abundant data gaps, especially in the austral winter months. This is caused by the signal here being very weak due to the low solar angle, resulting in very low signal/noise ratios. Additional data gaps may result from optical contamination by drifting ice in the marginal ice zone. Both issues cause pixels to be flagged and discarded during the image processing.

At high latitudes satellite data is scarce, due to cloud and ice cover, especially in the austral winter months, from June to August, where data scarcity occurs south of 45^{o}S. In contrast, in the months from January to March, data coverage extends down to 70^{o}S. This lack of data, especially in the winter, restricts predictions of DMS during this period. Additionally, no in situ DMS measurements are available in the winter months, therefore use of the algorithm developed in this work should potentially be restricted to the austral summer months only. It was also seen in figure 13b that there was a better correlation between M21 and K00 and L10 climatologies in the summer months than the winter months.

The peak of mean DMS concentration in June at latitudes between 40^{o}S and 50^{o}S, reflects a peak in both mean Chl and mean SST during this month, seen in figures 12b and c. This is not the normal expected behaviour of these variables at this time of the year. The actual occurrence of this DMS peak remains speculative because of the lack of in situ DMS data for this month. Moreover, it is important to note that satellite observations in June are unavailable south of 45^{o}S because of low solar elevation. Therefore, the average SST and chlorophyll for the 40-50^{o}S band reflects only data from its northernmost half. Additionally, inaccuracies in satellite measurements in the winter due to the low solar angle, may be the cause of the unexpected peaks in June.

In general, the M21 model has a positive bias for low in situ DMS concentrations, lower than 2 nmol L^{-1} approximately, and a negative bias for in situ DMS greater than 2 nmol L^{-1}. This behaviour can explain the tendency for too high DMS concentrations predicted by M21 in the austral winter when lowest DMS is typically expected, as in the L10 and K00 climatologies

5.3 Comparison to previous models

The algorithm developed in this work explains a greater statistical variance of DMS in the Southern Ocean than the previously developed empirical models**.** The most recent empirical model, G18 (Galí et al., 2018), on a global scale explained 56% of DMS variance. Comparison with G18 against L10 found that G18 has a strong regional bias in the Southern Ocean, leading to the underestimating of DMS in this region. The model developed in this work, M21, explains 67% variance for the Southern Ocean.

The mismatch in seasonal mean DMS between M21 and the climatologies K00 and L10, could be a result of lack of data from both sides. Lack of data impacts both the temporal and spatial structure of the climatologies. To make up for the missing data, estimates of monthly mean DMS concentration are done, however this is difficult due to the high temporal variability of DMS concentration. This can be particularly problematic for the seasonal evaluation in high latitudes. Low sampled areas, such as the Southern Ocean, can be influenced by large individual point measurements that are not representative of the whole month. Additionally, ocean regions can have large interannual variability, which is not considered in the construction of the climatology.

Some differences in latitudinal DMS behaviours comparing M21 against K00 and L10 could also be due to our exclusion of coastal waters, shallower than 1000m, which were not excluded in K00 nor L10.

5.4 Future challenges and model improvements

The algorithm developed could potentially be improved if more data was available. The number of in situ measurements are limited due harsh weather condition in the Southern Ocean, making research operations difficult in this region. The weather is especially harsh in the winter and the addition of sea ice means that no cruises are carried out during this period, resulting in an absence of data. Due to this, the developed algorithm should only be considered valid for the austral summer months, since there was only data available for these months.

There also exist limitations on the satellite matchup data, because cloud cover impedes the possibility of satellite measurements of the sea surface. Since the Southern Ocean is particularly cloudy compared to other ocean regions, it can occur that there are no satellite measurements available for certain in situ measurements. In this case this in situ measurement could not be used for developing the algorithm. Only about 10% of the in situ DMS data set had available matchups.

Further tuning could be carried out on the temperature boundary of 4^{o}C between the two temperature regimes. Tuning was only performed on integer values of temperature. Potentially the two models developed could be enhanced through more precise tuning.

There exists a discontinuity between the equations of the two temperature regimes. This can be seen clearly in the DMS maps in figure 11, approximately between 50^{o}S and 60^{o}S. As a future

improvement, the two equations could be made more continuous, making the boundary between the cold-wate regime and warm-water regime smoother.

The underestimation of DMS at high concentrations by the algorithm could possibly be improved using a parameter optimization approach that considers several statistical criteria simultaneously (Galí et al., 2018). Multiple linear regression is based solely on the minimization of RMSE, which often results in models with lower variance than the in situ reference data (Fig. 10), as shown by Jolliff et al. (2009). Such models typically overestimate in situ data in the low concentration range and underestimate them in the high concentration range. Better representation of DMS concentration extremes at high spatial resolution, which cannot be afforded by climatologies such as K00 and L10, could lead to better understanding of the radiative effects of DMS.

The observed patterns of DMS concentration in the Southern Ocean could be explained by its unique physical and biogeochemical characteristics. The low DMS concentrations in the 50^{o}S-60^{o}S latitude band could be a result of deep mixing depths of the ACC leading to light limitation, in addition to a deficiency in iron in this zone. This light-iron co-limitation would restrain the phytoplankton biomass in this zone, resulting in lower DMS concentrations. In contrast, close the land the DMS concentrations are higher, likely due to the fact that the mixing layer here is shallower and there is a greater availability of iron.

The influence of iron deficiency was not explored in this work since the developed algorithm was preferred to be satellite based only. Iron deficiency could however be a reason for why the previously developed global algorithms did not perform well for DMS prediction in the Southern Ocean.

Empirical estimation of Southern Ocean DMS distribution with the M21 algorithm can guide more detailed explorations of the mechanisms resulting in the observed DMS patterns. In turn, improved knowledge of these mechanisms can lead to further development of satellite algorithms. Ultimately DMS predicting algorithms will help to better understand the relationship between DMS producing phytoplankton and climate.

6. Conclusions

The algorithm developed in this work offers a satellite-based solution for the calculation of sea surface DMS in the Southern Ocean, opposed to previous models which also relied also on in situ data measurements.

The algorithm consists of two separate models for different temperature zones, the first model for a temperature range of -2^{o}C to 4^{o}C, and the second model from 4^{o}C to 18^{o}C.

The algorithm accounts for 67% of DMS variance in the open ocean, over depths greater than 1000m.

The general pattern of predicted DMS in the Southern Ocean shows high concentrations in the austral summer period and lower concentrations in the austral winter period.

The mean annual latitudinal DMS concentrations calculated with the algorithm developed in this work, shows a similar pattern to that of the climatologies of Kettle et al. (2000) and Lana et al. (2010), however seasonal means show less correlation, especially in the austral winter period.

The lack of available data in the Southern Ocean during the austral winter restricts the accuracy of prediction and validation of DMS concentration during this time period.

Achieving a better knowledge of DMS sea surface concentration consequently improves the prediction of marine DMS emissions into the atmosphere. Such knowledge can help to better understand the phytoplankton-climate feedback loop and its implications on the planet.

References

Alcolombri, U., Ben-Dor, S., Feldmesser, E., Levin, Y., Tawfik, D.S. and Vardi, A., 2015. Identification of the algal dimethyl sulphide–releasing enzyme: A missing link in the marine sulfur cycle. Science, 348(6242), pp.1466-1469.

Anderson, T.R., Spall, S.A., Yool, A., Cipollini, P., Challenor, P.G. and Fasham, M.J.R., 2001. Global fields of sea surface dimethylsulphide predicted from chlorophyll, nutrients and light. Journal of Marine Systems, 30(1-2), pp.1-20.

Andreae, M.O. and Rosenfeld, D., 2008. Aerosol–cloud–precipitation interactions. Part 1. The nature and sources of cloud-active aerosols. Earth-Science Reviews, 89(1-2), pp.13-41.

Aranami, K. and Tsunogai, S., 2004. Seasonal and regional comparison of oceanic and atmospheric dimethylsulphide in the northern North Pacific: Dilution effects on its concentration during winter. Journal of Geophysical Research: Atmospheres, 109(D12).

Ardyna, M., Claustre, H., Sallée, J.B., d'Ovidio, F., Gentili, B., van Dijken, G., d'Ortenzio, F. and Arrigo, K.R., 2017. Delineating environmental control of phytoplankton biomass and phenology in the Southern Ocean. Geophysical Research Letters, 44(10), pp.5016-5024.

Aumont, O., Belviso, S. and Monfray, P., 2002. Dimethylsulfoniopropionate (DMSP) and dimethylsulphide (DMS) sea surface distributions simulated from a global three-dimensional ocean carbon cycle model. Journal of Geophysical Research: Oceans, 107(C4), pp.4-1.

Belviso, S., Bopp, L., Moulin, C., Orr, J.C., Anderson, T.R., Aumont, O., Chu, S., Elliott, S., Maltrud, M.E. and Simó, R., 2004. Comparison of global climatological maps of sea surface dimethyl sulphide. Global Biogeochemical Cycles, 18(3).

Belviso, S., Masotti, I., Tagliabue, A., Bopp, L., Brockmann, P., Fichot, C., Caniaux, G., Prieur, L., Ras, J., Uitz, J. and Loisel, H., 2012. DMS dynamics in the most oligotrophic subtropical zones of the global ocean. Biogeochemistry, 110(1), pp.215-241.

Bodas-Salcedo, A., Williams, K.D., Ringer, M.A., Beau, I., Cole, J.N., Dufresne, J.L., Koshiro, T., Stevens, B., Wang, Z. and Yokohata, T., 2014. Origins of the solar radiation biases over the Southern Ocean in CFMIP2 models. Journal of Climate, 27(1), pp.41-56.

Bopp, L., Aumont, O., Belviso, S. and Monfray, P., 2003. Potential impact of climate change on marine dimethyl sulphide emissions. Tellus B: Chemical and Physical Meteorology, 55(1), pp.11-22.

Bristow, L.A., Mohr, W., Ahmerkamp, S. and Kuypers, M.M., 2017. Nutrients that limit growth in the ocean. Current Biology, 27(11), pp.R474-R478.

Carslaw, K.S., Lee, L.A., Reddington, C.L., Pringle, K.J., Rap, A., Forster, P.M., Mann, G.W., Spracklen, D.V., Woodhouse, M.T., Regayre, L.A. and Pierce, J.R., 2013. Large contribution of natural aerosols to uncertainty in indirect forcing. Nature, 503(7474), pp.67-71.

Carpenter, L.J., Archer, S.D. and Beale, R., 2012. Ocean-atmosphere trace gas exchange. Chemical Society Reviews, 41(19), pp.6473-6506.

Carter, L., McCave, I.N. and Williams, M.J., 2008. Circulation and water masses of the Southern Ocean: a review. Developments in earth and environmental sciences, 8, pp.85-114.

Chapman, C.C., Lea, M.A., Meyer, A., Sallée, J.B. and Hindell, M., 2020. Defining Southern Ocean fronts and their influence on biological and physical processes in a changing climate. Nature Climate Change, 10(3), pp.209-219.

Charlson, R.J., Lovelock, J.E., Andreae, M.O. and Warren, S.G., 1987. Oceanic phytoplankton, atmospheric sulphur, cloud albedo and climate. Nature, 326(6114), pp.655-661.

Collins, W.J., Bellouin, N., Doutriaux-Boucher, M., Gedney, N., Halloran, P., Hinton, T., Hughes, J., Jones, C.D., Joshi, M., Liddicoat, S. and Martin, G., 2011. Development and evaluation of an Earth-System model–HadGEM2. Geoscientific Model Development, 4(4), pp.1051-1075.

Curson, A.R., Todd, J.D., Sullivan, M.J. and Johnston, A.W., 2011. Catabolism of dimethylsulphoniopropionate: microorganisms, enzymes and genes. Nature Reviews Microbiology, 9(12), pp.849-859.

Elliott, S., 2009. Dependence of DMS global sea-air flux distribution on transfer velocity and concentration field type. Journal of Geophysical Research: Biogeosciences, 114(G2).

Flossmann, A.I. and Laj, P., 1998. Aerosols, gases and microphysics of clouds. EDP Sciences, Les Ulis, 1998) pp, pp.89-119.

Frölicher, T.L., Sarmiento, J.L., Paynter, D.J., Dunne, J.P., Krasting, J.P. and Winton, M., 2015. Dominance of the Southern Ocean in anthropogenic carbon and heat uptake in CMIP5 models. Journal of Climate, 28(2), pp.862-886.

Galí, M., Saló, V., Almeda, R., Calbet, A. and Simó, R., 2011. Stimulation of gross dimethylsulphide (DMS) production by solar radiation. Geophysical Research Letters, 38(15).

Galí, M., Devred, E., Levasseur, M., Royer, S.J. and Babin, M., 2015. A remote sensing algorithm for planktonic dimethylsulfoniopropionate (DMSP) and an analysis of global patterns. Remote Sensing of Environment, 171, pp.171-184.

Galí, M. and Simó, R., 2015. A meta-analysis of oceanic DMS and DMSP cycling processes: Disentangling the summer paradox. Global Biogeochemical Cycles, 29(4), pp.496-515.

Galí, M., Levasseur, M., Devred, E., Simó, R. and Babin, M., 2018. Sea-surface dimethylsulphide (DMS) concentration from satellite data at global and regional scales. Biogeosciences, 15(11), pp.3497-3519.

Hanley, K.E., Belcher, S.E. and Sullivan, P.P., 2010. A global climatology of wind–wave interaction. Journal of physical oceanography, 40(6), pp.1263-1282.

IPCC, 2014. Climate Change 2014 Synthesis Report. Contribution of working groups I. II and III to the fifth assessment report of the intergovernmental panel on climate change, 151(10.1017).

Jarníková, T. and Tortell, P.D., 2016. Towards a revised climatology of summertime dimethylsulphide concentrations and sea–air fluxes in the Southern Ocean. Environmental Chemistry, 13(2), pp.364-378.

Jolliff, J.K., Kindle, J.C., Shulman, I., Penta, B., Friedrichs, M.A., Helber, R. and Arnone, R.A., 2009. Summary diagrams for coupled hydrodynamic-ecosystem model skill assessment. Journal of Marine Systems, 76(1-2), pp.64-82.

Kameyama, S., Tanimoto, H., Inomata, S., Tsunogai, U., Ooki, A., Yokouchi, Y., Takeda, S., Obata, H. and Uematsu, M., 2009. Equilibrator inlet-proton transfer reaction-mass spectrometry (EI-PTR-MS) for sensitive, high-resolution measurement of dimethyl sulphide dissolved in seawater. Analytical chemistry, 81(21), pp.9021-9026.

Kameyama, S., Tanimoto, H., Inomata, S., Yoshikawa-Inoue, H., Tsunogai, U., Tsuda, A., Uematsu, M., Ishii, M., Sasano, D., Suzuki, K. and Nosaka, Y., 2013. Strong relationship between dimethyl sulphide and net community production in the western subarctic Pacific. Geophysical Research Letters, 40(15), pp.3986-3990.

Kettle, A.J., Andreae, M.O., Amouroux, D., Andreae, T.W., Bates, T.S., Berresheim, H., Bingemer, H., Boniforti, R., Curran, M.A.J., DiTullio, G.R. and Helas, G., 1999. A global database of sea surface dimethylsulphide (DMS) measurements and a procedure to predict sea surface DMS as a function of latitude, longitude, and month. Global Biogeochemical Cycles, 13(2), pp.399-444.

Kettle, A.J. and Andreae, M.O., 2000. Flux of dimethylsulphide from the oceans: A comparison of updated data sets and flux models. Journal of Geophysical Research: Atmospheres, 105(D22), pp.26793-26808.

Kim, Y.S. and Orsi, A.H., 2014. On the variability of Antarctic Circumpolar Current fronts inferred from 1992–2011 altimetry. Journal of Physical Oceanography, 44(12), pp.3054-3071.

Kloster, S., Feichter, J., Maier-Reimer, E., Six, K.D., Stier, P. and Wetzel, P., 2006. DMS cycle in the marine ocean-atmosphere system–a global model study. Biogeosciences, 3(1), pp.29-51.

Lana, A., Bell, T.G., Simó, R., Vallina, S.M., Ballabrera-Poy, J., Kettle, A.J., Dachs, J., Bopp, L., Saltzman, E.S., Stefels, J.J.G.B.C. and Johnson, J.E., 2011. An updated climatology of surface dimethlysulphide concentrations and emission fluxes in the global ocean. Global Biogeochemical Cycles, 25(1).

Landwehr, S., Volpi, M., Haumann, F.A., Robinson, C.M., Thurnherr, I., Ferracci, V., Baccarini, A., Thomas, J., Gorodetskaya, I., Tatzelt, C. and Henning, S., 2021. Biogeochemistry and Physics of the Southern Ocean-Atmosphere System Explored With Data Science. Earth System Dynamics Discussions, pp.1-114.

Marinov, I., Gnanadesikan, A., Toggweiler, J.R. and Sarmiento, J.L., 2006. The Southern Ocean biogeochemical divide. Nature, 441(7096), pp.964-967.

Maritorena, S. and Siegel, D.A., 2005. Consistent merging of satellite ocean color data sets using a bio-optical model. Remote Sensing of Environment, 94(4), pp.429-440.

McGillis, W.R., Dacey, J.W.H., Frew, N.M., Bock, E.J. and Nelson, R.K., 2000. Water-air flux of dimethylsulphide. Journal of Geophysical Research: Oceans, 105(C1), pp.1187-1193.

Miles, C.J., Bell, T.G. and Lenton, T.M., 2009. Testing the relationship between the solar radiation dose and surface DMS concentrations using in situ data. Biogeosciences, 6(9), pp.1927-1934.

Miles, C.J., Bell, T.G. and Suntharalingam, P., 2012. Investigating the inter-relationships between water attenuated irradiance, primary production and DMS (P). Biogeochemistry, 110(1), pp.201-213.

Quinn, P.K. and Bates, T.S., 2011. The case against climate regulation via oceanic phytoplankton sulphur emissions. Nature, 480(7375), pp.51-56.

Ooki, A., Nomura, D., Nishino, S., Kikuchi, T. and Yokouchi, Y., 2015. A global-scale map of isoprene and volatile organic iodine in surface seawater of the A rctic, N orthwest P acific, I ndian, and S outhern O ceans. Journal of Geophysical Research: Oceans, 120(6), pp.4108-4128.

Orsi, A.H., Whitworth III, T. and Nowlin Jr, W.D., 1995. On the meridional extent and fronts of the Antarctic Circumpolar Current. Deep Sea Research Part I: Oceanographic Research Papers, 42(5), pp.641-673.

Pollard, R.T., Lucas, M.I. and Read, J.F., 2002. Physical controls on biogeochemical zonation in the Southern Ocean. Deep Sea Research Part II: Topical Studies in Oceanography, 49(16), pp.3289-3305.

Rintoul, S.R. and Garabato, A.C.N., 2013. Dynamics of the Southern Ocean circulation. In International Geophysics (Vol. 103, pp. 471-492). Academic Press.

Rodríguez-Ros, P., Cortés, P., Robinson, C.M., Nunes, S., Hassler, C., Royer, S.J., Estrada, M., Sala, M.M. and Simó, R., 2020. Distribution and drivers of marine isoprene concentration across the Southern Ocean. Atmosphere, 11(6), p.556.

Saltzman, E.S., De Bruyn, W.J., Lawler, M.J., Marandino, C.A. and McCormick, C.A., 2009. A chemical ionization mass spectrometer for continuous underway shipboard analysis of dimethylsulphide in near-surface seawater. Ocean Science, 5(4), pp.537-546.

Simó, R., 2001. Production of atmospheric sulfur by oceanic plankton: biogeochemical, ecological and evolutionary links. Trends in Ecology & Evolution, 16(6), pp.287-294.

Simó, R. and Dachs, J., 2002. Global ocean emission of dimethylsulphide predicted from biogeophysical data. Global Biogeochemical Cycles, 16(4), pp.26-1.

Six, K.D. and Maier-Reimer, E., 2006. What controls the oceanic dimethylsulphide (DMS) cycle? A modeling approach. Global biogeochemical cycles, 20(4).

Sokolov, S. and Rintoul, S.R., 2007. On the relationship between fronts of the Antarctic Circumpolar Current and surface chlorophyll concentrations in the Southern Ocean. Journal of Geophysical Research: Oceans, 112(C7).

Stefels, J., Steinke, M., Turner, S., Malin, G. and Belviso, S., 2007. Environmental constraints on the production and removal of the climatically active gas dimethylsulphide (DMS) and implications for ecosystem modelling. Biogeochemistry, 83(1), pp.245-275.

Tesdal, J.E., Christian, J.R., Monahan, A.H. and von Salzen, K., 2015. Evaluation of diverse approaches for estimating sea-surface DMS concentration and air–sea exchange at global scale. Environmental Chemistry, 13(2), pp.390-412.

Thomas, M.A., Suntharalingam, P., Pozzoli, L., Rast, S., Devasthale, A., Kloster, S., Feichter, J. and Lenton, T.M., 2010. Quantification of DMS aerosol-cloud-climate interactions using the ECHAM5-HAMMOZ model in a current climate scenario. Atmospheric Chemistry and Physics, 10(15), pp.7425-7438.

Thomas, M.A., Suntharalingam, P., Pozzoli, L., Rast, S., Devasthale, A., Kloster, S., Feichter, J. and Lenton, T.M., 2010. Quantification of DMS aerosol-cloud-climate interactions using the ECHAM5-HAMMOZ model in a current climate scenario. Atmospheric Chemistry and Physics, 10(15), pp.7425-7438.

Tortell, P.D., 2005. Dissolved gas measurements in oceanic waters made by membrane inlet mass spectrometry. Limnology and Oceanography: Methods, 3(1), pp.24-37.

Vallina, S.M. and Simó, R., 2007. Strong relationship between DMS and the solar radiation dose over the global surface ocean. Science, 315(5811), pp.506-508.

Vogt, M. and Liss, P.S., 2009. Dimethylsulphide and climate. Surface Ocean-Lower Atmosphere Processes, edited by: Le Quéré, C., and Saltzman, ES, American Geophysical Union, Washington, DC, pp.197-232.

Vogt, M., Vallina, S.M., Buitenhuis, E.T., Bopp, L. and Le Quéré, C., 2010. Simulating dimethylsulphide seasonality with the dynamic green ocean model PlankTOM5. Journal of Geophysical Research: Oceans, 115(C6).

Wanninkhof, R., 1992. Relationship between wind speed and gas exchange over the ocean. Journal of Geophysical Research: Oceans, 97(C5), pp.7373-7382.